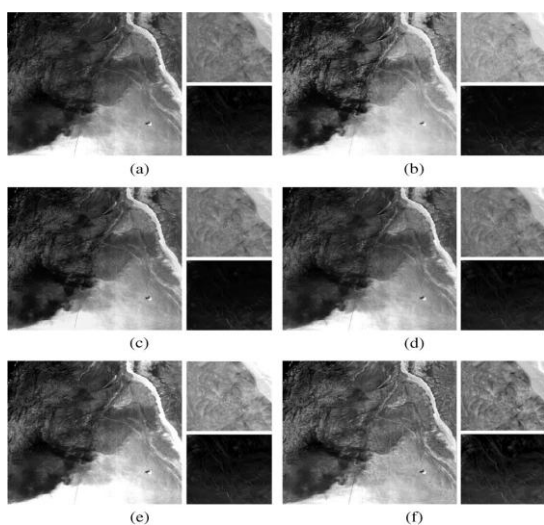


**Figure 3:** (a) Knee transfer functions for three layers using the corresponding knee points and sp line interpolation.  $b_l$  and  $b_h$  represent low and high bounds, respectively, of intensity  $O, x$ , and  $\Delta$  represent low, middle and high intensity layers, respectively. (b) Adaptive intensity transfer functions for three layers.

Since remote sensing images have spatially varying intensity distributions, we estimate the optimal transfer function in each brightness range for adaptive contrast enhancement. The adaptive transfer function is estimated by using the knee transfer and the gamma adjustment functions. For the global contrast enhancement, the knee transfer function stretches the low-intensity range by determining knee points according to the dominant brightness of each layer as shown in Fig. 3(a).

#### 4. Experimental Results

For evaluating the performance of the proposed algorithm, we tested three low-contrast remote sensing images as shown in Figs. 4–6(a). The performance of the proposed algorithm is compared with existing well-known algorithms including standard HE, RMSHE, GC-CHE, and Demirel’s methods. For the experiment, we used  $\gamma = 1.4$ ,  $b_l = 0.4$ , and  $b_h = 0.7$ . For three different intensity layers,  $w_l = 1$ ,  $w_m = 3$ , and  $w_h = 1$  were used.


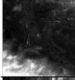
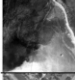



**Figure 4:** (a) Original satellite image from KARI; contrast-enhanced images by using (b) the standard HE, (c) RMSHE, (d) GC-CHE, (e) Demirel’s, and (f) the proposed methods

Figs. 4–5 show the results of contrast enhancement using the standard HE, RMSHE, GC-CHE, Demirel’s, and the

proposed methods. As shown in Figs. 4–5(b), the results of the standard HE method show under- or oversaturation artifacts because It can not maintain the average brightness level. Although RMSHE and GC-CHE methods can preserve the average brightness level, and better enhance overall image quality, they lost edge details in low- and high-intensity ranges as shown in Figs. 4–5(c) and (d). On the other hand, Demirel’s method could not sufficiently enhance the low-intensity range as shown in Figs. 4–5(e) because of the singular-value constraint of the target image. Figs. 4–5(f) show the results of the proposed contrast enhancement method. The overall image quality is significantly enhanced with preserving the average brightness level and edge details in all intensity ranges. For performance evaluation, we used the measure of enhancement (EME) which is computed.

**Table 1:** Eme Values Of Five Different Enhancement methods

	Standard HE [1]	RMSHE [4]	GC-CHE [5]	Demirel’s method [6]	Proposed method
	0.025	0.010	0.125	0.764	0.786
	1.172	4.978	1.173	2.732	2.746
	1.023	0.944	0.965	1.944	2.126
	0.689	0.680	0.838	0.626	0.703

#### 5. Conclusion

In this letter, we have presented a novel contrast enhancement method for remote sensing images using dominant brightness analysis and adaptive intensity transformation. The proposed algorithm decomposes the input image into four wavelet sub bands and decomposes the LL sub band into low, middle and high-intensity layers by analyzing the log-average luminance of the corresponding layer. The adaptive intensity transfer functions are computed by combining the knee transfer function and the gamma adjustment function. All the contrast-enhanced layers are fused with an appropriate smoothing, and the processed LL band undergoes the IDWT together with unprocessed LH, HL, and HH sub bands. The proposed algorithm can effectively enhance the overall quality and visibility of local details better than existing state-of-the-art methods including RMSHE, GC-CHE, and Demirel’s methods. Experimental results demonstrate that the proposed algorithm can enhance the low-contrast satellite images and is suitable for various imaging devices such as consumer camcorders, real-time 3-D reconstruction systems, and computational cameras.

#### References

- [1] R. Gonzalez and R. Woods, *Digital Image Processing*, 3rd ed. Englewood Cliffs, NJ: Prentice-Hall, 2007.
- [2] Y. Kim, “Contrast enhancement using brightness preserving bi-histogram equalization,” *IEEE Trans. Consum. Electron.*, vol. 43, no. 1, pp. 1–8, Feb. 1997.

- [3] Y. Wan, Q. Chen, and B. M. Zhang, "Image enhancement based on equal area dualistic sub-image histogram equalization method," *IEEE Trans. Consum. Electron.*, vol. 45, no. 1, pp. 68–75, Feb. 1999.
- [4] S. Chen and A. Ramli, "Contrast enhancement using recursive meanseparate histogram equalization for scalable brightness preservation," *IEEE Trans. Consum. Electron.*, vol. 49, no. 4, pp. 1301–1309, Nov. 2003.
- [5] T. Kim and J. Paik, "Adaptive contrast enhancement using gain controllable clipped histogram equalization," *IEEE Trans. Consum. Electron.*, vol. 54, no. 4, pp. 1803–1810, Nov. 2008.
- [6] H. Demirel, C. Ozcinar, and G. Anbarjafari, "Satellite image contrast enhancement using discrete wavelet transform and singular value decomposition," *IEEE Geosci. Remote Sens. Lett.*, vol. 7, no. 2, pp. 333–337, Apr. 2010.
- [7] H. Demirel, G. Anbarjafari, and M. Jahromi, "Image equalization based on singular value decomposition," in *Proc. 23rd IEEE Int. Symp. Comput. Inf. Sci.*, Istanbul, Turkey, Oct. 2008, pp. 1–5.
- [8] E. Reinhard, M. Stark, P. Shirley, and J. Ferwerda, "Photographic tone reproduction for digital images," in *Proc. SIGGRAPH Annu. Conf. Comput. Graph.*, Jul. 2002, pp. 249–256.
- [9] L. Meylan and S. Susstrunk, "High dynamic range image rendering with aretinex-based adaptive filter," *IEEE Trans. Image Process.*, vol. 15, no. 9, pp. 2820–2830, Sep. 2006.
- [10] S. Chen and A. Beghdadi, "Nature rendering of color image based on retinex," in *Proc. IEEE Int. Conf. Image Process.*, Nov. 2009, pp. 1813–1816.
- [11] Y. Monobe, H. Yamashita, T. Kurosawa, and H. Kotera, "Dynamic range compression preserving local image contrast for digital video camera," *IEEE*